Research Article Vol. 1, No. 1 / July 2014 / Optica 10

Microresonator frequency comb optical clock

Scott B. Papp,[1,*] Katja Beha,[1] Pascal Del'Haye,[1] Franklyn Quinlan,[1] Hansuek Lee,[2] Kerry J. Vahala,[2] and Scott A. Diddams[1]

[1]Time and Frequency Division 688, National Institute of Standards and Technology, Boulder, Colorado 80305, USA

[2]T. J. Watson Laboratory of Applied Physics, California Institute of Technology, Pasadena, California 91125, USA

*Corresponding author: scott.papp@nist.gov

Received 4 April 2014; revised 16 June 2014; accepted 17 June 2014 (Doc. ID 209505); published 22 July 2014

Optical frequency combs serve as the clockwork of optical clocks, which are now the best time-keeping systems in existence. The use of precise optical time and frequency technology in various applications beyond the research lab remains a significant challenge, but one that integrated microresonator technology is poised to address. Here, we report a silicon-chip-based microresonator comb optical clock that converts an optical frequency reference to a microwave signal. A comb spectrum with a 25 THz span is generated with a 2 mm diameter silica disk and broadening in nonlinear fiber. This spectrum is stabilized to rubidium frequency references separated by 3.5 THz by controlling two teeth 108 modes apart. The optical clock's output is the electronically countable 33 GHz microcomb line spacing, which features stability better than the rubidium transitions by the expected factor of 108. Our work demonstrates the comprehensive set of tools needed for interfacing microcombs to state-of-the-art optical clocks.

OCIS codes: (140.3945) Microcavities; (190.4410) Nonlinear optics, parametric processes; (230.4910) Oscillators.

http://dx.doi.org/10.1364/OPTICA.1.000010

1. INTRODUCTION

Optical frequency combs enable extraordinary measurement precision and accuracy entirely commensurate with their reference oscillator. A new direction in experiments is the creation of ultracompact combs via parametric nonlinear optics in microresonators [1,2]. We refer to these as microcombs, and here we report a silicon-chip-based microcomb optical clock that phase-coherently converts an optical reference to a microwave signal.

Optical clocks leverage the narrow, unvarying transitions of atoms to realize exceptionally stable laser frequencies measured at below the 10^{-17} level [3]. Optical frequency combs facilitate the measurement and use of these atomic references by providing a set of clock-referenced lines that span more than an octave [4]. Moreover, they have enabled advances in diverse fields from spectroscopy of atoms and molecules [5,6] to astronomy [7].

A new type of frequency comb has emerged based on optical microresonators [1,2]. Here, the comb generation relies on nonlinear parametric oscillation and cascaded four-wave mixing driven by a CW laser. Such microcombs offer revolutionary advantages over existing comb technology, including chip-based photonic integration, uniquely large comb-mode spacings in the tens of gigahertz range, and monolithic construction with small size and power consumption. Microcomb development has included frequency control of their spectra [8–11], characterization of their noise properties [12–14], a Rb-stabilized microcomb oscillator [15], and demonstration of phase-locked [12,16,17] and mode-locked states [18,19]. However, the milestone of all-optical frequency control of a microcomb to an atomic reference, including frequency division to the microwave domain, has not been achieved.

In this paper, we report the achievement of this goal by demonstrating a functional optical clock based on full stabilization of a microcomb to atomic Rb transitions. We generate a low-noise, continuously equidistant microcomb spectrum by use of an on-chip silica microresonator. The clock output is the 33 GHz microcomb line spacing, which is electronically measurable, and a traceable integer partition of the 3.5 THz frequency spacing of the Rb references. Here, we explore the basic features of this microcomb clock. Its 5×10^{-9} Allan

deviation for 1 s averaging is completely dominated by the Rb reference, and the microcomb contribution is only $<2 \times 10^{-14}$ at 1 s, indicating that much more stable clocks could be supported. Our results highlight an architecture for the integration of microcombs with other high-performance and chip-scale atomic frequency references [20].

2. EXPERIMENTAL METHODS

Figure 1(a) shows a schematic of our microcomb optical clock. A 2 mm diameter disk resonator with a 10° wedge side profile provides parametric comb generation. The resonator, which has an unloaded quality factor of 63 million, is fabricated on a silicon chip using conventional semiconductor fabrication techniques [21]. Hence, the core of our system is scalable and could be integrated with other on-chip photonic elements, and eventually atomic systems [20,22]. In these experiments we use a tapered fiber for evanescent coupling [23]. We excite the disk resonator with light from a CW laser (optical frequency ν_p) that is intensity modulated at frequency f_{eo} and amplified to a maximum of 140 mW. The first-order sideband powers are approximately 3 dB lower than the pump, and the piece of highly nonlinear fiber (HNLF) before the disk resonator increases the second-order (third-order) sidebands to 12 (25) dB below the pump. The modulation implements our parametric seeding technique [11], which enables unmatched control of the microcomb line spacing. Here we further demonstrate that parametric seeding enables the complete suppression of undesirable, nonequidistant subcombs. Following generation in the disk resonator, the microcomb output is optically filtered to attenuate the pump laser and modulation sidebands; the resulting spectrum is shown by the top trace in Fig. 1(b). The microcomb bandwidth is approximately a factor of 10 higher than the seeding comb. By amplifying the microcomb spectrum and without any dispersion control, we broaden the initial 20 nm bandwidth an additional factor of 10 to 200 nm. The ~2 ps duration optical waveform obtained directly from the microresonator offers sufficient peak power for our experiments and is stable and repeatable even for different settings of pump frequency and power, intensity modulation, taper–resonator coupling, and pump polarization. The broadened spectrum [Fig. 1(b)] overlaps with the resonance frequencies of molecules such as HCN, C_2H_2, CO_2, CH_4, and atomic Rb and K after second-harmonic generation.

For frequency stabilization, we heterodyne the microcomb spectrum with telecom-grade semiconductor distributed feedback (DFB) lasers at 1560 and 1590 nm. These lasers are frequency doubled and stabilized to well-known Rb transitions [24–26]. Precise Rb spectroscopic data, especially near 780 nm, exist, and with attention to systematic effects a stability of $10^{-12}/\sqrt{\tau}$ has been demonstrated [24]. Therefore, we focus only on salient details for controlling the microcomb with these optical references. To operate an optical clock, we stabilize the microcomb's two *independent* degrees of freedom to the Rb references by leveraging frequency control of its spectrum. The central line of the microcomb is phase locked to the 1560 nm DFB laser, which is separate from the pump laser. [9,15]. Additionally, the 108th comb line from the center, which we obtain via spectral broadening, is phase locked to the 1590 nm DFB laser by tuning the microcomb line spacing through control of f_{eo}.

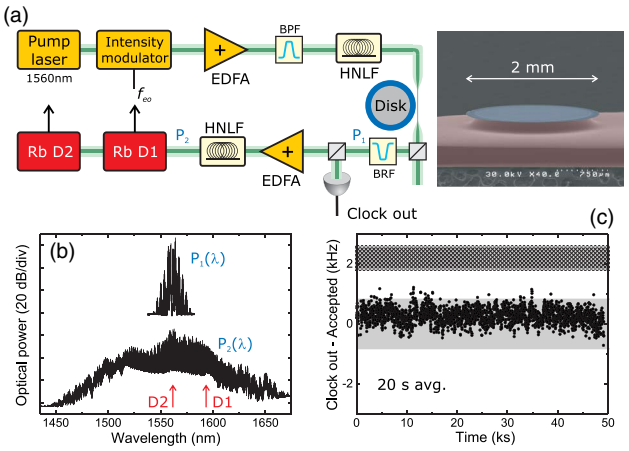

Fig. 1. Microcomb optical clock with Rb atoms. (a) An intensity-modulated pump laser excites a chip-based microresonator (see micrograph at right) to create a 33 GHz spacing comb. The comb is broadened in highly nonlinear fiber (HNLF) following amplification to 1.4 W. Two lines of the comb 108 modes apart are stabilized to Rb transitions by control of the pump frequency and the intensity modulation f_{eo}. The clock output is obtained via photodetection of the unbroadened spectrum. Not shown are polarization controllers, which are needed before the intensity modulator, the microresonator, the HNLF, and all the elements of the Rb spectrometers. Other components are an optical bandpass filter (BPF), a bandreject filter (BRF), and two erbium-doped fiber amplifiers (EDFA). (b) Optical spectrum after a filter to suppress the pump (top) and following spectral broadening (bottom), (c) optical clock output over 12 h. Each point is the average of twenty 1 s measurements. For comparison, published Rb spectroscopic data on the D2–D1 difference divided by 108 has been subtracted. The solid [25] and hatched [26] gray regions represent previous data.

3. RESULTS AND DISCUSSION

The output of our microcomb optical clock is obtained via photodetection of the $\Delta\nu = 32.9819213$ GHz line spacing, which reflects the frequency difference Δ_{Rb} of the D2- and D1-stabilized lasers divided by 108, and a fixed 660/108 MHz offset for phase stabilization. This specific offset arises because the comb's central mode is phase locked at a frequency 920 MHz higher than the 1560 nm laser, while mode 108 is phase locked 260 MHz higher than the 1590 nm laser. The offset could assume a range of predetermined values, including zero, and the microresonator free spectral range could be targeted to utilize a specific value. The data points in Fig. 1(c) are a continuous >12 h long record of the clock output. Here, the vertical axis shows the difference between the clock output and $\Delta_{Rb} = 3,561,387,470(180)$ kHz, whose uncertainty [24–26] is shown by the gray band. Although we have not systematically analyzed the accuracy of our clock, its output is in reasonable agreement with these previous data. The 271 Hz RMS fluctuation in a 20 s average of the clock output is significantly reduced from those of the D2 and D1 reference lasers, due to the principle of optical frequency division associated with

frequency combs [4,27,28]. The remainder of this paper presents an investigation of our clock, including the deterministic generation of an equidistant microcomb spectrum, a demonstration of the precise relationship between the clock output and Rb reference, and an analysis of the clock's stability.

The essential aspect of a frequency comb is a uniform spacing of all its modes. However, microcomb spectra are often composed of overlapping subcombs with different offset frequencies [29]. Such a microcomb spectrum has a fundamentally reduced frequency measurement precision and is unusable for our optical clock experiment. Subcombs arise when parametric oscillation creates initial signal/idler fields in resonator modes $\pm m_i$ away from the one excited by the pump laser. The green lines in Fig. 2(a) show a schematic of a subcomb with characteristic frequency offset from that of an equidistant comb given by $\nu_0 = n_1(\Delta P - m_i \Delta\nu)$, where $\Delta P \approx m_i \Delta\nu$ is the primary spacing with order n_1. We use a coherent control technique, parametric seeding, to deterministically suppress subcombs and favor a continuous comb with a single offset frequency. The seeding comb, whose spectrum $\nu_m = \nu_p + m f_{eo}$ is shown by the red lines in Fig. 2(a), experiences parametric gain in the microresonator, and it induces sidebands of the first signal/idler pair that fix $\Delta\nu$ of all parametrically generated lines at f_{eo}. In this paper, we demonstrate for the first time (to our knowledge) that sufficient amplitude of the seeding comb $\nu_{\pm m_i}$ modes can injection lock the subcomb, which completely nullifies its frequency offset ν_0.

To investigate subcomb injection-locking (Fig. 2), we monitor the amplitudes of subcomb and parametric seeding comb lines while we tune f_{eo}, and thus ν_0. Information about these amplitudes is obtained via photodetection of the entire microcomb spectrum, which yields a signal at frequency $\Delta\nu$ and its sidebands associated with ν_0; see the schematic in Fig. 2(b). The measurement of RF power versus frequency in Fig. 2(c) shows $\Delta\nu$ and ν_0, including its four-wave mixing harmonics. By recording many such traces for different settings of f_{eo}, we explore the transition into and out of injection-locked operation; Fig. 2(d) presents a false color "waterfall" plot of these data. Here the horizontal band at zero is the microcomb line spacing, which is always f_{eo}, and the other bands are associated with the subcomb offset. As the offset is tuned toward zero via a computer-controlled scan of f_{eo} in 1.7 kHz increments, we observe an abrupt suppression of the subcomb RF components. This represents the point at which the line frequencies of the seeding comb and subcomb are sufficiently close to capture the latter. A linear fit of the first-order offset signals yields the f_{eo} setting (this fit establishes f_{lock}) for $\nu_0 = 0$, which is used to calibrate the horizontal axis of Fig. 2(d), and the slope, which corresponds to m_i. The injection-locking range is 400 kHz, in which the RF frequencies associated with the subcomb offset are suppressed by >40 dB; see Fig. 2(c). In future experiments, such a large locking range would enable a direct harmonic relationship between Δ_{Rb} and $\Delta\nu$. Following initiation of the injection-locked state, the microcomb's spectrum is equidistant and offset free and can operate continuously for >24 h. (The seeding must remain on.) We verify the equidistance of the central 110 lines of the broadened microcomb spectrum by use of a calibrated reference system [11].

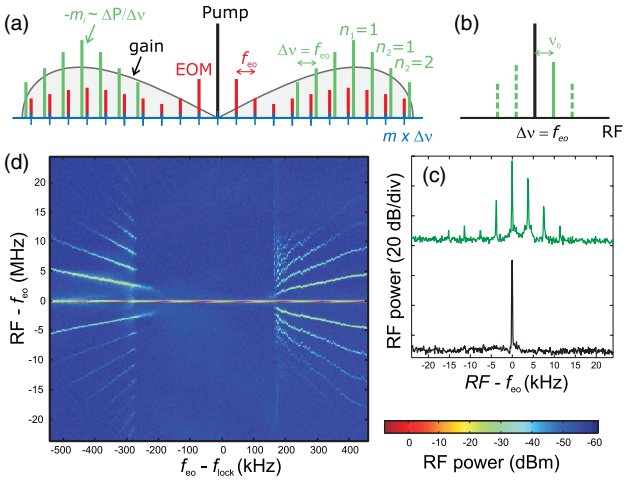

Fig. 2. Injection locking to create an equidistant microcomb. (a) Model for microcomb generation, including a subcomb (green) and parametric seeding (red), (b) model RF spectrum after photodetection. All the comb lines contribute at frequency $\Delta\nu = f_{eo}$, and the presence of a subcomb is reflected in the sidebands spaced by ν_0. (c) Measured RF spectra with a 100 kHz resolution bandwidth, indicating a subcomb (top, green) with $\nu_0 \approx 4$ MHz at $f_{eo} - f_{lock} = -387$ kHz and an injection-locked comb (bottom, black) at $f_{eo} = f_{lock}$, (d) waterfall plot compiled from many traces like those in (c). The false color bar shows the scaling of RF power.

Our microcomb optical clock is designed to generate an electronically detectable microwave output at a precise *integer* subdivision of the Rb reference. In contrast to earlier work [15], the clock output is traceable to atomic structure without regard to the operating parameters or conditions of the microcomb. To test this principle, we simultaneously count the DFB lasers' frequencies and the clock output and characterize their degree of correlation. The frequencies are recorded in nearly continuous 1 s intervals by use of an auxiliary self-referenced and repetition-rate-stabilized Er:fiber frequency comb [30]. In Fig. 3(a), the black points show the clock output, while the red open points are $\Delta_{Rb}/108$. Since the difference of the DFB lasers is not calibrated, for clarity we subtract its mean value $\bar{\Delta}_{Rb}/108$ from all the points. The overlap of the two data sets suggests their correlation, which we analyze in more detail by plotting them against each other; see Fig. 3(b). A linear fit of this correlation plot yields a slope of 108.0002(59), and the horizontal intercept differs from zero by only -2.4 ± 1.5 Hz, compared to the ~3.5 THz frequency of the Rb reference. Knowledge of Δ_{Rb} via the stabilized fiber comb enables us to compare the clock signal with its optical reference in real time. Figure 3(c) shows a frequency counter record of the clock output from the same dataset as in Fig. 1(c), but here at each point a correction for the noise of the Rb spectrometers is applied. This reduces the scale of clock fluctuations by a factor of ~1000 to the hertz level and demonstrates that they are overwhelmingly determined by the Rb reference.

We expect the microcomb clock output will closely reproduce the frequency stability of the Rb references. To characterize them, we record the optical heterodyne frequency of the microcomb and the 1590 nm laser, while the microcomb's

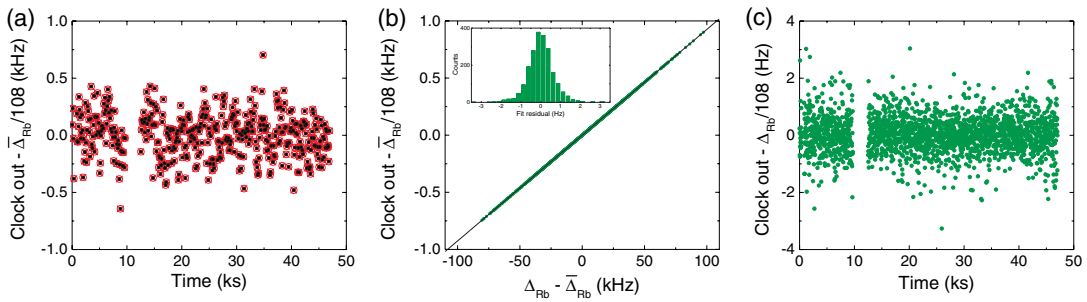

Fig. 3. Subdivision of the 3.5 THz Rb reference. (a) Clock output (black points) and difference of the Rb-stabilized DFB lasers (red circles) minus the mean of all Δ_{Rb} measurements. Here, 100-sample mean values of the 1 s gate data are displayed. (b) Strong correlation of clock output and the terahertz frequency of the Rb reference. The inset shows a histogram of the fit residuals. (c) Real-time-corrected clock output with 0.64 Hz standard deviation. During the gap in measurements at 10 ks, the fiber comb was unlocked.

central line is phase locked to the 1560 nm laser. For this experiment, the phase lock to the 1590 nm laser is switched off and a constant parametric seeding frequency, which is synthesized from a hydrogen maser, determines the microcomb line spacing. The open circles in Fig. 4 show the combined Allan deviation of the Rb references normalized to 33 GHz for six decades of integration time. For short measurement periods the stability increases as approximately $1/\sqrt{\tau}$. However near 0.1 s the Allan deviation increases and only slowly improves for averaging periods up to 10,000 s. The impact of systematic drifts on the Rb transitions due to, for example, excitation laser power fluctuations, magnetic field noise, and the Rb vapor cell pressure has been discussed extensively in the literature [24]. Importantly, these effects, rather than any associated with the microcomb, explain the references' stability.

With microcomb servo control via the Rb D1 reference restored, we analyze the clock output by way of its Allan deviation, which is obtained with respect to a synthesized 33 GHz frequency referenced to a hydrogen maser. Importantly, the clock's stability (filled black points in Fig. 4) is improved by a factor of ~100 over that of the DFB lasers, whose noise is distributed among all the lines of the microcomb. Such

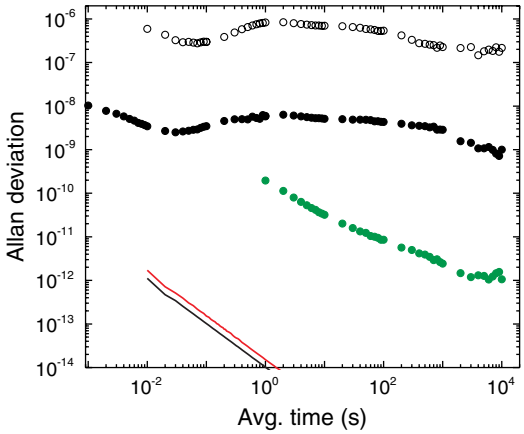

Fig. 4. Microcomb optical clock stability. Allan deviation of the DFB lasers (open points) and the microcomb clock (closed black points) normalized to a 33 GHz carrier. The green points are the clock stability after correcting the Rb reference noise via measurements against an auxiliary comb. The red and black traces represent the in-loop residual noise for stabilization of the microcomb pump laser and mode 108, respectively.

optical frequency division is the key metrological feature of any comb. Fluctuations and inaccuracy of the Rb-referenced lasers are naturally reflected in the microcomb clock output, and this explains the slow averaging of the black filled points in Fig. 4 beyond ~0.1 s. On the other hand, the in-loop noise of the two servos that stabilize the microcomb, which are shown by the black and red traces in Fig. 4, indicate that our microcomb system as currently configured could support more stable frequency references, and hence produce a 33 GHz output with a 1 s fractional stability of 2×10^{-14}. Increasing the bandwidth of the servo loops, in particular by shortening the second HNLF, would improve residual noise. We demonstrate this potential for improvement by characterizing the clock output, including its real-time correction for Rb reference noise [Fig. 3(c)]. The green points in Fig. 4 show an upper limit for the corrected clock output's Allan deviation, which monotonically decreases with averaging time to 10^{-12} at 10,000 s. Accordingly, we project that a microcomb utilizing compact, all-optical Rb frequency references in a controlled environment [24] could produce a 33 GHz output with $5 \times 10^{-11}/\sqrt{\tau}$ stability.

4. CONCLUSION

In conclusion, we have reported the all-optical stabilization of a chip-based microresonator frequency comb to atomic Rb transitions. The electronically detectable microwave output of our optical clock is stable, and it accurately subdivides the terahertz frequency difference of the Rb references. At present the clock output stability is limited entirely by the Rb references. However, the microcomb frequency control architecture demonstrated here is sufficient to support references with orders-of-magnitude-higher performance. Future work will address this point, as well as focus on generation of higher-peak-power optical waveforms directly from the microcomb. Combined with nonlinear spectral broadening, this would enable the subdivision of even larger frequency gaps and ultimately the self-referencing of a microcomb.

FUNDING INFORMATION

Defense Advanced Research Projects Agency (DARPA) (PULSE, QuASAR), National Aeronautics and Space Administration (NASA), Air Force Office of Scientific Research (AFOSR), and Kavli NanoScience Institute at Caltech.

ACKNOWLEDGMENTS

We thank Elizabeth Donley and Andrew Ludlow for thoughtful comments on this manuscript and M. Hirano for supplying the HNLF. It is a contribution of the U.S. government (NIST) and is not subject to copyright in the United States of America.

REFERENCES

1. P. Del'Haye, A. Schliesser, O. Arcizet, T. Wilken, R. Holzwarth, and T. J. Kippenberg, "Optical frequency comb generation from a monolithic microresonator," Nature **450**, 1214–1217 (2007).
2. T. J. Kippenberg, R. Holzwarth, and S. A. Diddams, "Microresonator-based optical frequency combs," Science **332**, 555–559 (2011).
3. N. Hinkley, J. A. Sherman, N. B. Phillips, M. Schioppo, N. D. Lemke, K. Beloy, M. Pizzocaro, C. W. Oates, and A. D. Ludlow, "An atomic clock with 10^{-18} instability," Science **341**, 1215–1218 (2013).
4. S. A. Diddams, T. Udem, J. C. Bergquist, E. A. Curtis, R. E. Drullinger, L. Hollberg, W. M. Itano, W. D. Lee, C. W. Oates, K. R. Vogel, and D. J. Wineland, "An optical clock based on a single trapped $^{199}Hg^{+}$ ion," Science **293**, 825–828 (2001).
5. K.-K. Ni, S. Ospelkaus, M. H. G. de Miranda, A. Pe'er, B. Neyenhuis, J. J. Zirbel, S. Kotochigova, P. S. Julienne, D. S. Jin, and J. Ye, "A high phase-space-density gas of polar molecules," Science **322**, 231–235 (2008).
6. M. J. Thorpe, K. D. Moll, R. J. Jones, B. Safdi, and J. Ye, "Broadband cavity ringdown spectroscopy for sensitive and rapid molecular detection," Science **311**, 1595–1599 (2006).
7. M. T. Murphy, T. Udem, R. Holzwarth, A. Sizmann, L. P. C. Araujo-Hauck, H. Dekker, S. D'Odorico, M. Fischer, T. W. Hansch, and A. Manescau, "High-precision wavelength calibration of astronomical spectrographs with laser frequency combs," Mon. Not. R. Astron. Soc. **380**, 839–847 (2007).
8. P. Del'Haye, O. Arcizet, A. Schliesser, R. Holzwarth, and T. J. Kippenberg, "Full stabilization of a microresonator-based optical frequency comb," Phys. Rev. Lett. **101**, 053903 (2008).
9. S. B. Papp, P. Del'Haye, and S. A. Diddams, "Mechanical control of a microrod-resonator optical frequency comb," Phys. Rev. X **3**, 031003 (2013).
10. P. Del'Haye, S. B. Papp, and S. A. Diddams, "Hybrid electro-optically modulated microcombs," Phys. Rev. Lett. **109**, 263901 (2012).
11. S. B. Papp, P. Del'Haye, and S. A. Diddams, "Parametric seeding of a microresonator optical frequency comb," Opt. Express **21**, 17615–17624 (2013).
12. S. B. Papp and S. A. Diddams, "Spectral and temporal characterization of a fused-quartz-microresonator optical frequency comb," Phys. Rev. A **84**, 053833 (2011).
13. A. A. Savchenkov, E. Rubiola, A. B. Matsko, V. S. Ilchenko, and L. Maleki, "Phase noise of whispering gallery photonic hyperparametric microwave oscillators," Opt. Express **16**, 4130–4144 (2008).
14. J. Li, H. Lee, T. Chen, and K. J. Vahala, "Low-pump-power, low-phase-noise, and microwave to millimeter-wave repetition rate operation in microcombs," Phys. Rev. Lett. **109**, 233901 (2012).
15. A. A. Savchenkov, D. Eliyahu, W. Liang, V. S. Ilchenko, J. Byrd, A. B. Matsko, D. Seidel, and L. Maleki, "Stabilization of a Kerr frequency comb oscillator," Opt. Lett. **38**, 2636–2639 (2013).
16. F. Ferdous, H. Miao, D. E. Leaird, K. Srinivasan, J. Wang, L. Chen, L. T. Varghese, and A. M. Weiner, "Spectral line-by-line pulse shaping of on-chip microresonator frequency combs," Nat. Photonics **5**, 770–776 (2011).
17. P. Del'Haye, K. Beha, S. B. Papp, and S. A. Diddams, "Self-Injection locking and phase-locked states in microresonator-based optical frequency combs," Phys. Rev. Lett. **112**, 043905 (2014).
18. T. Herr, V. Brasch, J. D. Jost, C. Y. Wang, N. M. Kondratiev, M. L. Gorodetsky, and T. J. Kippenberg, "Temporal solitons in optical microresonators," Nat. Photonics **8**, 145–152 (2014).
19. K. Saha, Y. Okawachi, B. Shim, J. S. Levy, R. Salem, A. R. Johnson, M. A. Foster, M. R. E. Lamont, M. Lipson, and A. L. Gaeta, "Modelocking and femtosecond pulse generation in chip-based frequency combs," Opt. Express **21**, 1335–1343 (2013).
20. S. Knappe, V. Gerginov, P. D. D. Schwindt, V. Shah, H. G. Robinson, L. Hollberg, and J. Kitching, "Atomic vapor cells for chip-scale atomic clocks with improved long-term frequency stability," Opt. Lett. **30**, 2351–2353 (2005).
21. H. Lee, T. Chen, J. Li, K. Y. Yang, S. Jeon, O. Painter, and K. J. Vahala, "Chemically etched ultrahigh-*Q* wedge-resonator on a silicon chip," Nat. Photonics **6**, 369–373 (2012).
22. W. Yang, D. B. Conkey, B. Wu, D. Yin, A. R. Hawkins, and H. Schmidt, "Atomic spectroscopy on a chip," Nat. Photonics **1**, 331–335 (2007).
23. M. Cai, O. Painter, and K. J. Vahala, "Observation of critical coupling in a fiber taper to silica-microsphere whispering gallery mode system," Phys. Rev. Lett. **85**, 74–77 (2000).
24. J. Ye, S. Swartz, P. Jungner, and J. L. Hall, "Hyperfine structure and absolute frequency of the ^{87}Rb $5P_{3/2}$ state," Opt. Lett. **21**, 1280–1282 (1996).
25. A. Marian, M. C. Stowe, J. R. Lawall, D. Felinto, and J. Ye, "United time-frequency spectroscopy for dynamics and global structure," Science **306**, 2063–2068 (2004).
26. M. Maric, J. J. McFerran, and A. N. Luiten, "Frequency-comb spectroscopy of the D1 line in laser-cooled rubidium," Phys. Rev. A **77**, 32502 (2008).
27. W. C. Swann, E. Baumann, F. R. Giorgetta, and N. R. Newbury, "Microwave generation with low residual phase noise from a femtosecond fiber laser with an intracavity electro-optic modulator," Opt. Express **19**, 24387–24395 (2011).
28. T. M. Fortier, M. S. Kirchner, F. Quinlan, J. Taylor, J. C. Bergquist, T. Rosenband, N. Lemke, A. Ludlow, Y. Jiang, C. W. Oates, and S. A. Diddams, "Generation of ultrastable microwaves via optical frequency division," Nat. Photonics **5**, 425–429 (2011).
29. T. Herr, K. Hartinger, J. Riemensberger, W. C. Y. E. Gavartin, R. L. Holzwarth, M. Gorodetsky, and T. J. Kippenberg, "Universal formation dynamics and noise of Kerr-frequency combs in microresonators," Nat. Photonics **6**, 480–487 (2012).
30. F. Quinlan, T. M. Fortier, M. S. Kirchner, J. A. Taylor, M. J. Thorpe, N. Lemke, A. D. Ludlow, Y. Jiang, and S. A. Diddams, "Ultralow phase noise microwave generation with an Er:fiber-based optical frequency divider," Opt. Lett. **36**, 3260–3262 (2011).